

A. Corsini · F. Rispoli · A. Santoriello · T.E. Tezduyar

Improved discontinuity-capturing finite element techniques for reaction effects in turbulence computation

Received: 28 December 2005 / Accepted: 22 January 2006 / Published online: 21 February 2006
© Springer-Verlag 2006

Abstract Recent advances in turbulence modeling brought more and more sophisticated turbulence closures (e.g. $k-\varepsilon$, $k-\varepsilon-v^2-f$, Second Moment Closures), where the governing equations for the model parameters involve advection, diffusion and reaction terms. Numerical instabilities can be generated by the dominant advection or reaction terms. Classical stabilized formulations such as the Streamline-Upwind/Petrov-Galerkin (SUPG) formulation (Brook and Hughes, *comput methods Appl Mech Eng* 32:199–255, 1982; Hughes and Tezduyar, *comput methods Appl Mech Eng* 45:217–284, 1984) are very well suited for preventing the numerical instabilities generated by the dominant advection terms. A different stabilization however is needed for instabilities due to the dominant reaction terms. An additional stabilization term, called the diffusion for reaction-dominated (DRD) term, was introduced by Tezduyar and Park (*comput methods Appl Mech Eng* 59:307–325, 1986) for that purpose and improves the SUPG performance. In recent years a new class of variational multi-scale (VMS) stabilization (Hughes, *comput methods Appl Mech Eng* 127:387–401, 1995) has been introduced, and this approach, in principle, can deal with advection-diffusion-reaction equations. However, it was pointed out in Hanke (*comput methods Appl Mech Eng* 191:2925–2947) that this class of methods also need some improvement in the presence of high reaction rates. In this work we show the benefits of using the DRD operator to enhance the core stabilization techniques such as the SUPG and VMS formulations. We also propose a new operator called the DRDJ (DRD with the local variation jump) term, targeting

the reduction of numerical oscillations in the presence of both high reaction rates and sharp solution gradients. The methods are evaluated in the context of two stabilized methods: the classical SUPG formulation and a recently-developed VMS formulation called the V-SGS (Corsini et al. *comput methods Appl Mech Eng* 194:4797–4823, 2005). Model problems and industrial test cases are computed to show the potential of the proposed methods in simulation of turbulent flows.

Keywords Finite element · Variational method · Discontinuities

1 Introduction

The objective in this paper is to provide improved finite element formulations capable of dealing with advection-diffusion-reaction equations. For advection-dominated problems, a number of stabilized formulations such as the SUPG method [3,16] are available, which are quite effective in preventing the spurious numerical oscillations. Reaction-dominated problems, on the other hand, still need improved methods that are more effective in preventing the numerical oscillations, and, as stated in [1], this is so even in the context of the recently-developed variational multi-scale (VMS) methods. Thus there is still need for good numerical techniques for equations appearing in advanced turbulence models, combustion and chemistry. The diffusion for reaction-dominated (DRD) formulation was proposed in [2], which involves adding diffusion where reaction is dominant with respect to advection or diffusion.

The work here is based on using the DRD concept as a discontinuity-capturing tool, so that diffusion is added only when the reaction rates and solution gradients are both high. This is accomplished in the context of the Streamline-Upward/Petrov-Galerkin (SUPG) [3] and V-SGS [4] formulations. The objective in the approach we take here is to accomplish the additional stabilization without affecting the accuracy in advection-dominated zones and in zones where the solution is smooth. The main application area in the present work is turbomachinery CFD, with emphasis on advanced

A. Corsini (✉) · F. Rispoli · A. Santoriello
Department of Mechanics and Aeronautics
University of Rome “La Sapienza”
Via Eudossiana 18, Rome, I00184, Italy
E-mail: alessandro.corsini@uniroma1.it
E-mail: franco.rispoli@uniroma1.it
E-mail: a.santoriello@dma.ing.uniroma1.it

T.E. Tezduyar
Mechanical Engineering, Rice University
MS 321 6100 Main Street, Houston, TX 77005, USA
E-mail: tezduyar@rice.edu

turbulence closure models within the Reynolds-averaged Navier–Stokes (RANS) approach. We are focusing on addressing the numerical challenges posed by the reaction terms appearing in the closure equations of eddy viscosity models, such as the k - ε or k - ε - v^2 - f models [5].

Reaction-dominated zones are not uncommon in turbulent flows and in turbomachinery. For example, in stagnating and re-circulating flow zones the flow velocity approaches zero and the reaction effects dominate the advection and diffusion effects. Recent studies [6] have shown that application of a reaction-dependent residual scheme to the RANS equations with eddy-viscosity closures enables a realistic representation of turbulence in turbomachinery flows.

In Sect. 2, we provide an overview of the original DRD method and the DRDJ method as a version that takes into account the local “jump” in the solution. We also describe in that section how the DRD and DRDJ methods are applied to advection–diffusion–reaction problems. In Sect. 3, by using the model problem proposed in [2], the numerical performances of the DRD and DRDJ methods are assessed in conjunction with the SUPG and V-SGS formulations. In Sect. 4, we apply the DRDJ method, again in conjunction with the SUPG and V-SGS formulations, to 2D flow computation in a compressor cascade with controlled-diffusion blade profile, where we use the k - ε - v^2 - f turbulence model [5].

2 DRD and DRDJ techniques

The closure equations used in some turbulence models exhibit an advection–diffusion–reaction form, which in a 1D framework can be written as

$$B\phi + u\phi_{,x} - \kappa\phi_{,xx} = 0. \quad (2.1)$$

The discrete counterpart of the exact solution of the problem has an exponential behavior, characterized by two of the following three dimensionless parameters:

$$Pe = \frac{uh}{2\kappa}, \quad (2.2)$$

$$\beta^2 = \frac{B}{\kappa} \left(\frac{h}{2}\right)^2, \quad \gamma = \frac{Bh}{u}, \quad (2.3)$$

where h is the element length used in the calculations. The dimensionless parameter given by Eq. (2.2) represents the significance of the advection effects relative to the diffusion effects. The two parameters given by Eq. (2.3) represent the significance of the reaction effects relative to the diffusion and advection effects, respectively. While the stabilization methods such as the SUPG and V-SGS formulations are effective in addressing the numerical challenges encountered as Pe tends to large values, a DRD-like stabilization enhancement improves the solution when β^2 or γ becomes large.

2.1 Diffusion for reaction-dominated method

The original DRD method [2] proposed for the diffusion–reaction and advection–reaction equations involves numeri-

cal diffusion terms expressed as functions of, respectively, the first and second dimensionless parameters given by Eq. (2.3). In advection–reaction problems, the expression for the numerical diffusivity is given in [2] as

$$\tilde{\kappa}_{AR}(\gamma) = \frac{1}{2}uh(-\coth\gamma + \gamma(1/\sinh^2\gamma + 4r)), \quad (2.4)$$

where r is determined by the integration rule used in integrations over element domains (e.g. $r = 1/6$ for the two-point Gaussian quadrature rule and $r = 0$ for the “lumped” case).

The multi-dimensional extension is obtained in [2] by defining a numerical diffusivity tensor as follows:

$$\tilde{\kappa} = \tilde{\kappa}_{AR}(\gamma)\mathbf{ss} + \tilde{\kappa}_{AR}(\infty)(\mathbf{tt} + \mathbf{vv}), \quad (2.5)$$

where \mathbf{s} is the unit vector along the streamline, \mathbf{t} and \mathbf{v} are unit vectors orthogonal to \mathbf{s} and each other, and (2.4) is calculated with $|\mathbf{u}|$ instead of u . The element length scale h is defined in [2] as

$$h = h_{UGN} = 2 \left(\sum_a |\mathbf{s} \cdot \nabla N_a| \right)^{-1} \quad (2.6)$$

An expression for the numerical diffusivity in diffusion–reaction problems is also given in [2]:

$$\tilde{\kappa}_{DR}(\beta) = B(h/2)^2(4r + 1/\sinh^2\beta - 1/\beta^2), \quad (2.7)$$

with the multi-dimensional element length scale defined as given by Eq. (2.6). In the multi-dimensional extension here, however, we propose to use the diffusive length scale given in [7]:

$$h = h_{RGN} = 2 \left(\sum_a |\mathbf{r} \cdot \nabla N_a| \right)^{-1} \quad (2.8)$$

with \mathbf{r} defined as the unit vector in the direction of the solution gradient:

$$\mathbf{r} = \frac{\nabla \|\mathbf{u}\|}{\|\nabla \|\mathbf{u}\|\|}. \quad (2.9)$$

It was pointed out in [2] that the reaction-dominated limits of Eqs. (2.4) and (2.7) are the same:

$$\tilde{\kappa}_{AR}(\infty) = \tilde{\kappa}_{DR}(\infty) = 4rB(h/2)^2. \quad (2.10)$$

2.2 Diffusion for reaction-dominated term with local variation, jump (DRDJ)

We propose a new version of the DRD, which we call the DRDJ, that takes into account the local variation (“jump”) in the solution. This concept is similar to the one used in discontinuity-capturing directional dissipation technique [7]. The DRDJ diffusivities for the advection–reaction and diffusion–reaction equations are given as follows:

$$\tilde{\kappa}_{AR}(\gamma, J_e) = \frac{1}{2}uh_{UGN}J_e(-\coth\gamma + \gamma(1/\sinh^2\gamma + 4r)), \quad (2.11a)$$

$$\tilde{\kappa}_{\text{DR}}(\beta, J_e) = B(h_{\text{RGN}}/2)^2 J_e (4r + 1/\sinh^2 \beta - 1/\beta^2), \quad (2.11b)$$

where J_e is a normalized measure of the variation (“jump”) in the solution over an element e .

In the multi-dimensional version of the DRDJ the diffusivity tensor is given as:

$$\tilde{\kappa} = \tilde{\kappa}_{\text{AR}}(\gamma, J_e) \mathbf{ss} + \tilde{\kappa}_{\text{DR}}(\beta, J_e) (\mathbf{tt} + \mathbf{vv}). \quad (2.12)$$

Remark 1 The parameter J_e is defined as

$$J_e = \frac{(\phi_{\max})_e - (\phi_{\min})_e}{\|\phi\|_e}, \quad (2.13)$$

with $(\phi_{\max})_e$ and $(\phi_{\min})_e$ denoting the maximum and minimum values of ϕ in element, respectively. Here $\|\phi\|_e$ represents the scaling associated with element e , which can be calculated locally, or can be set globally, as it is done in Sect. 3. Turbulent flows involve flow parameters with different orders of magnitudes in different zones of the flow field. Therefore in turbulent flow computations $\|\phi\|_e$ is calculated locally. It can be set to the maximum value of ϕ in the element, as it is done in the calculations reported in Sect. 4. For $\phi > 0$ this choice assures that J_e ranges from 0 to 1. We note that in the \mathbf{t} and \mathbf{v} directions the numerical diffusivity is the one associated with the diffusion–reaction case.

Remark 2 Typically the closure equations of turbulence models are in the form of advection–diffusion–reaction equations. However it is not uncommon to also find diffusion–reaction equations governing elliptic parameters such as the \tilde{f} in the k - ε - v^2 - f model. In such cases the DRDJ expression is given as follows:

$$\tilde{\kappa}_e = \tilde{\kappa}_{\text{DR}}(\beta, J_e) \mathbf{I}, \quad (2.14)$$

where \mathbf{I} is the identity tensor.

In this paper the DRD and DRDJ are used in conjunction with the SUPG [3] and V-SGS [4] formulations. The V-SGS formulation was developed starting from the VMS method recently proposed by Hughes [8] and Hughes et al. [9]. The VMS approach introduces the additional feature of controlling the reactive effects, but, as pointed out in [1], this class of methods still need some improvement in the presence of high reaction rates.

3 Scalar test problem

This test problem was first proposed in [2] to evaluate the performance of the original DRD formulation. The governing equations are given as follows:

$$5\phi + u\phi_{,x} = 0,$$

$$u(y) = u_{\max}(1 - y^2), \quad (3.1)$$

$$u_{\max} = 1.$$

The discretization is based on a nonuniform Cartesian grid with 40×20 linear finite elements. Figure 1 shows the problem geometry, boundary conditions and the mesh.

Figure 2 shows the exact solution and the solutions obtained with the following methods: SUPG, SUPG plus mass lumping (SUPG+ML), SUPG plus DRD (SUPG+DRD), SUPG plus DRDJ (SUPG+DRDJ), V-SGS, V-SGS plus DRD (VSGS+DRD), and V-SGS plus DRDJ (VSGS+DRDJ).

The SUPG formulation results in the largest oscillations, while the V-SGS formulation, with its additional feature of controlling the reaction effects, significantly reduces the oscillations. Mass lumping results in a solution that is too diffusive. The DRD and DRDJ enhancements do very well in reducing the oscillations, especially when they are used in conjunction with the V-SGS stabilization. Figures 3, 4 and 5, respectively show the solution profiles at the first, second and third rows of nodes at and near the boundary where $y = 1$, $u = 0$, and the reaction terms are most significant.

The SUPG solution profile exhibits a 57% undershoot along the first row of nodes. That is reduced to less than 20% in the SUPG+DRD and SUPG+DRDJ profiles. Mass lumping yields a profile that is too diffusive. Along the same row of nodes, the V-SGS, V-SGS+DRD and V-SGS+DRDJ profiles all very comparable and also very close to the exact solution. Along the second row of nodes, the SUPG profile continues to have some undershoot, which is reduced significantly in the SUPG+DRD and SUPG+DRDJ profiles. Again, mass lumping yields a profile that is too diffusive. The V-SGS profile shows a 25% undershoot along this row nodes, but the undershoot is completely eliminated in the V-SGS+DRD and V-SGS+DRDJ profiles. The V-SGS+DRDJ profile is closer to the exact solution. Along the third row of nodes, all profiles, except for the one obtained with the SUPG+ML approach, are very close to the exact solution. Mass lumping leads to a profile that is too diffusive and far from the exact solution.

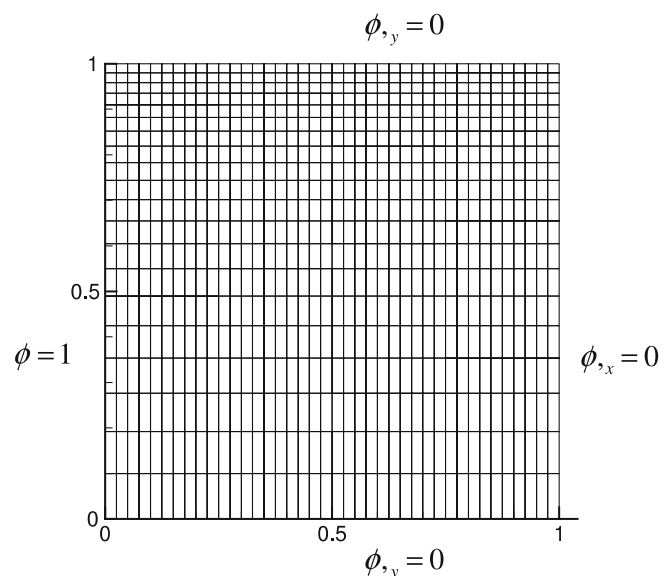


Fig. 1 Scalar test problem. Problem geometry, boundary conditions and mesh (40×20 elements)

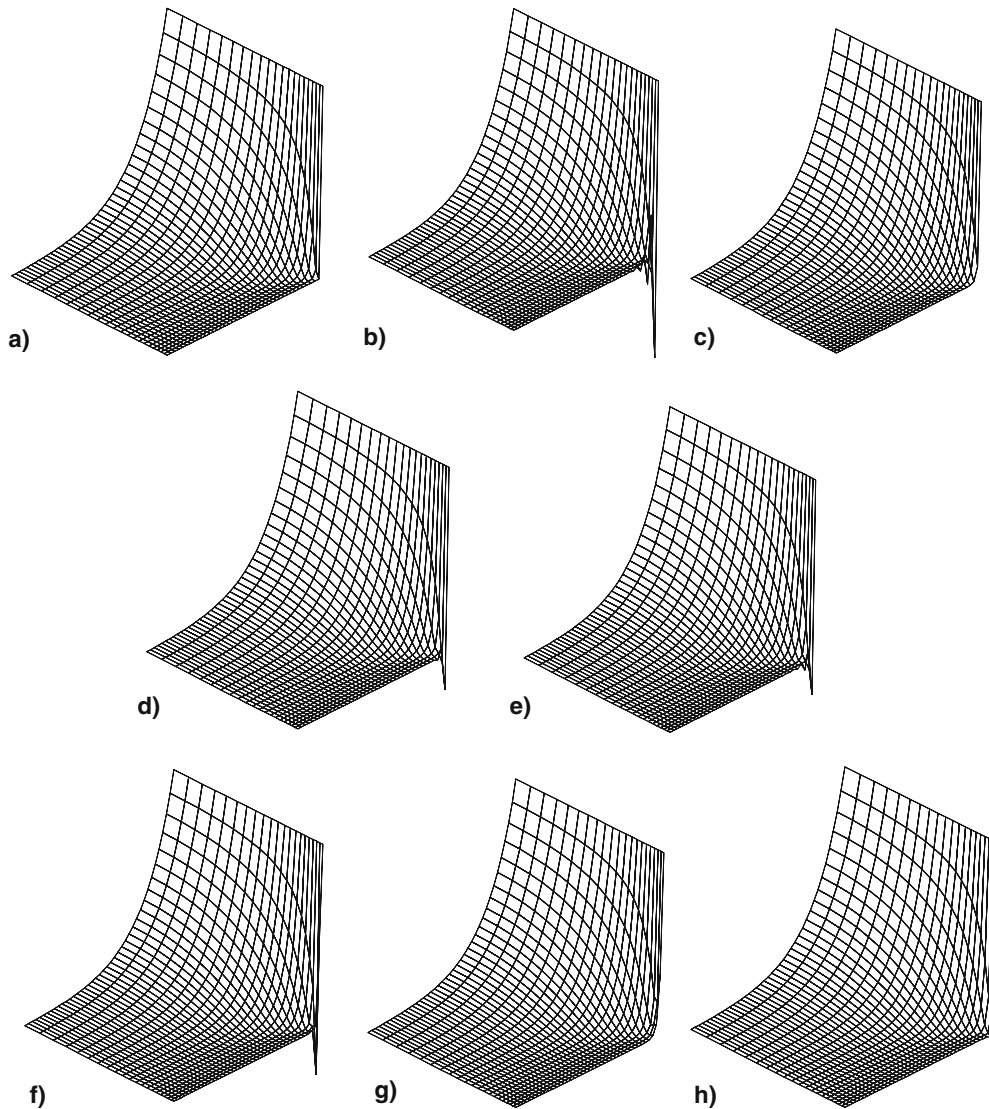


Fig. 2 Scalar test problem. **a** exact solution, and solutions obtained with the following methods: **(b)** SUPG, **(c)** SUPG+ML, **(d)** SUPG+DRD, **(e)** SUPG+DRDJ, **(f)** V-SGS, **(g)** V-SGS+DRD, and **(h)** V-SGS+DRDJ

From this test problem we conclude that in advection–reaction problems with reaction-dominated zones, the DRD and DRDJ enhancements significantly improve the solutions when used in conjunction with the SUPG and V-SGS stabilizations. Although the V-SGS formulation without DRD or DRDJ enhancements yields solutions better than the SUPG formulation without such enhancements, it still benefits substantially from either of these enhancements. We also conclude that the mass lumping approach is far from being ideal.

4 Turbulent flow test problem: controlled-diffusion compressor cascade

4.1 k - ε - v^2 - f turbulence closure

The turbulence closure used here is the k - ε - v^2 - f model first proposed by Durbin [10]. The inclusion of the variable $\overline{v^2}$,

regarded as the turbulence stress normal to the streamlines, brings improvements in simulation of turbomachinery flows. This is because of the role turbulence fluctuations in the wall-normal direction play in the transitional boundary layers. The computations are carried out based on the code-friendly version of the turbulence model [5], which uses on solid walls homogeneous Dirichlet boundary conditions for a modified elliptic relaxation variable, namely \tilde{f} .

The equations for the turbulent kinetic energy k , homogeneous dissipation rate $\tilde{\varepsilon} = \varepsilon - D$, turbulence stress normal to the streamlines $\overline{v^2}$, and the elliptic relaxation variable \tilde{f} are written as follows:

$$\overline{u_i} k_{,i} - \left[\left(\nu + \frac{\nu_t}{\sigma_k} \right) k_{,i} \right]_{,i} + B_k k = P_k + D, \quad (4.1)$$

$$\overline{u_i} \tilde{\varepsilon}_{,i} - \left[\left(\nu + \frac{\nu_t}{\sigma_\varepsilon} \right) \tilde{\varepsilon}_{,i} \right]_{,i} + B_\varepsilon \tilde{\varepsilon} = C_{\varepsilon 1} \frac{\tilde{\varepsilon}}{k} P_k, \quad (4.2)$$

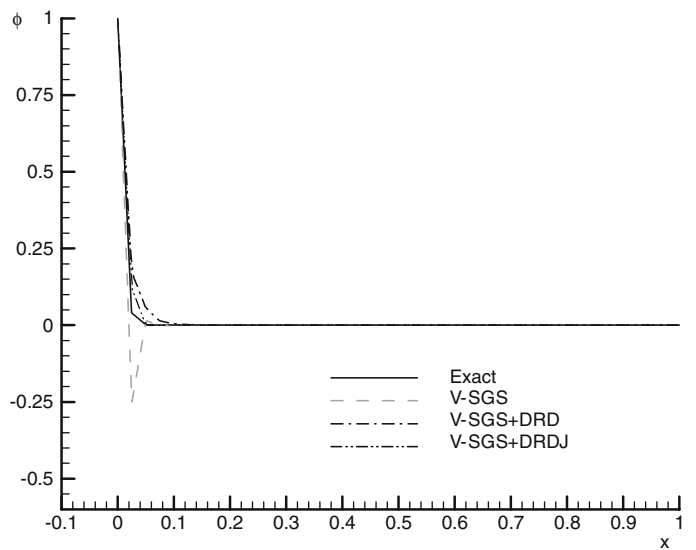
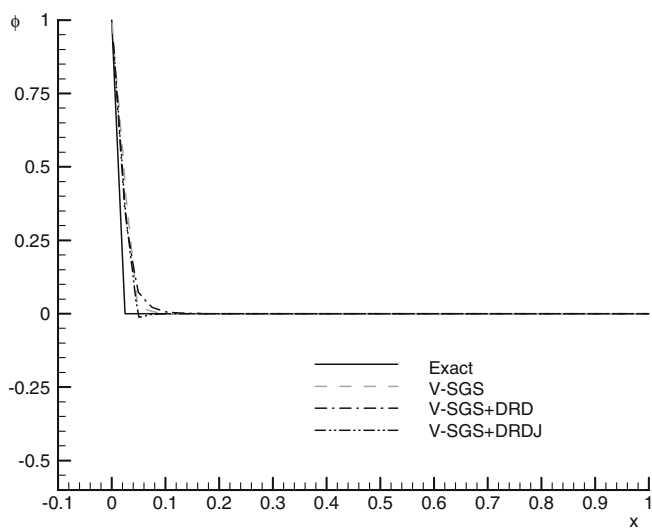
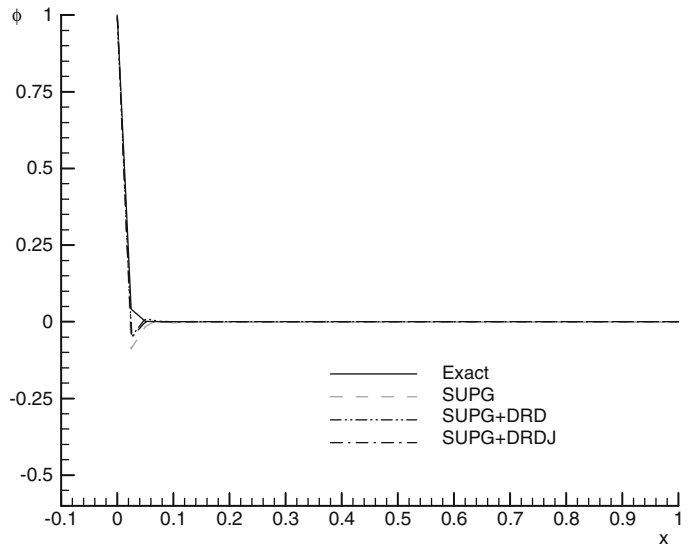
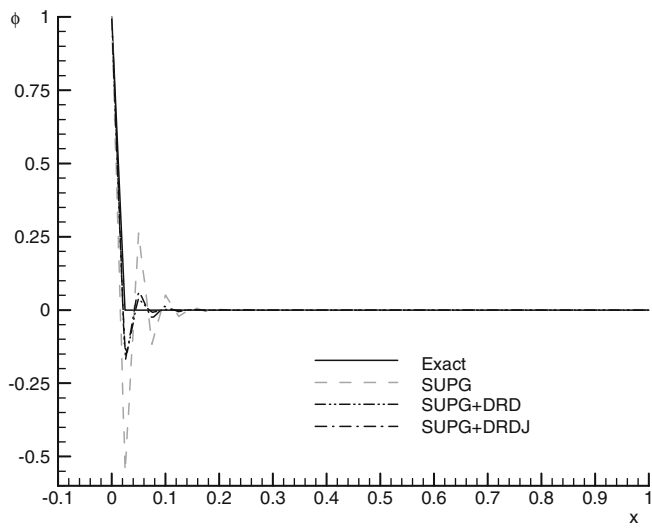
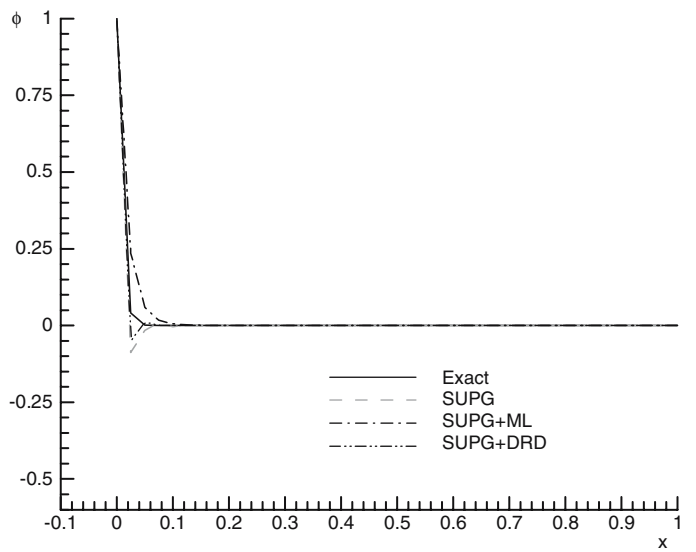
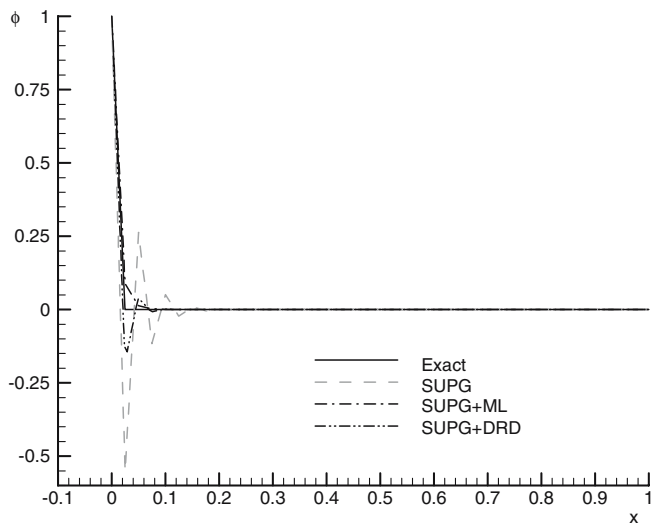


Fig. 3 Scalar test problem. Solution profiles at the first row of nodes ($y=1$)

Fig. 4 Scalar test problem. Solution profiles at the second row of nodes

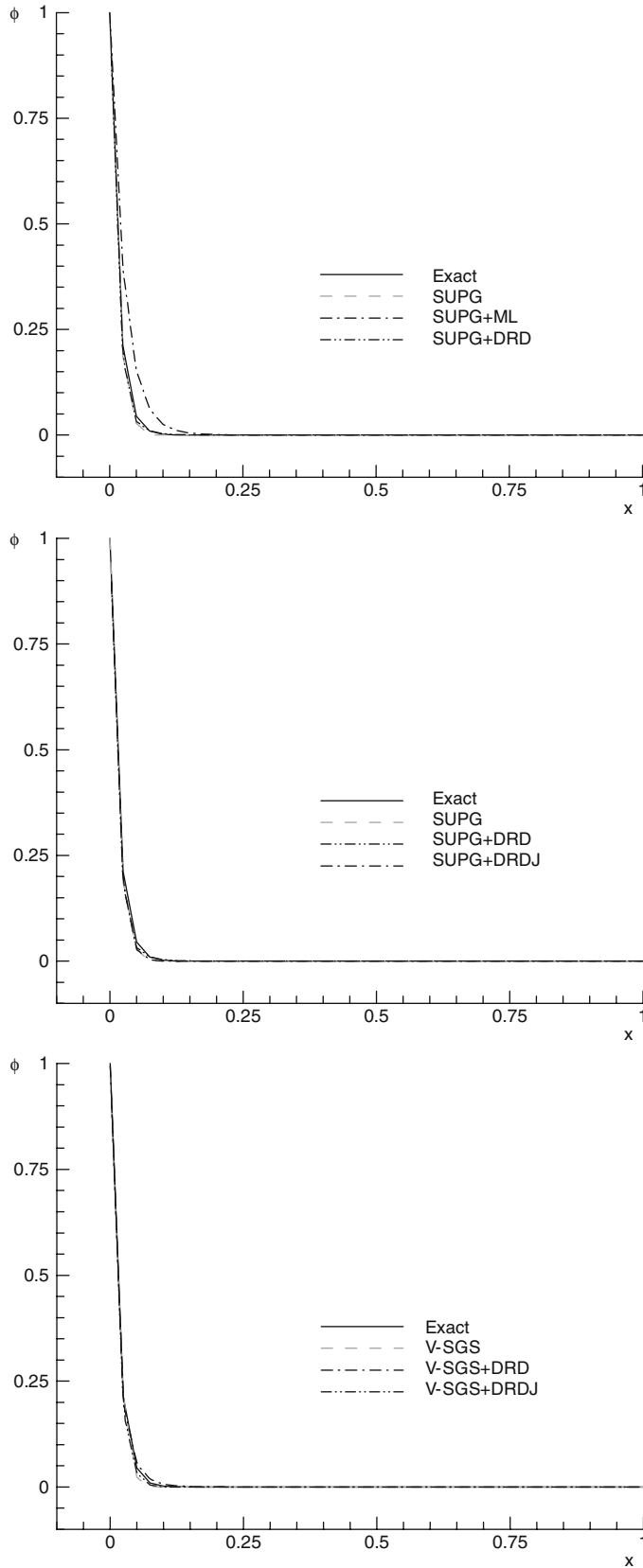


Fig. 5 Scalar test problem. Solution profiles at the third row of nodes

$$\bar{u}_i \bar{v}^{\prime 2},_i - \left[\left(v + \frac{v_t}{\sigma_k} \right) \bar{v}^{\prime 2},_i \right],_i + B_{v2} \bar{v}^{\prime 2} = k \tilde{f}, \quad (4.3)$$

$$- \left(L_s^2 \tilde{f},_i \right),_i + B_f \tilde{f} = C_2 \frac{P_k}{k} + (C_1 - 1) \left(\frac{\bar{v}^{\prime 2}}{k} - \frac{2}{3} \right) \frac{1}{T_s} + \frac{\bar{v}^{\prime 2}}{k} \frac{5}{T_s}, \quad (4.4)$$

where an overbar denotes the Reynolds-averaged quantities and a prime denotes the fluctuations. The Reynolds stress-strain relation is modeled according to a linear Boussinesq approximation:

$$\overline{u'_i u'_j} = \frac{2}{3} k \delta_{ij} - \nu_t S_{ij}, \quad (4.5)$$

where δ_{ij} is the Kronecker delta, $S_{ij} = (\bar{u}_{i,j} + \bar{u}_{j,i})$ is twice the strain-rate tensor, and the eddy viscosity is expressed as

$$\nu_t = c_\mu \bar{v}^{\prime 2} \frac{k}{\tilde{\epsilon}}. \quad (4.6)$$

Table 1 lists the closure coefficients for the code-friendly version of the k - ϵ - v^2 - f model [5].

4.2 Results

The test case is a 2D compressor cascade model with controlled-diffusion blade profile, experimentally studied by Elazar and Shreeve [11] using a two-component LDV system. The blade profile has a 14.4° stagger angle, the cascade solidity is 1.67, and the chord length $l_c = 127.3$ mm. Only

Table 1 Closure coefficients for the k - ϵ - v^2 - f model

P_k	$\overline{u'_i u'_k} \bar{u}_{i,k}$
D	$2\nu(\partial\sqrt{k}/\partial x_i)^2$
C_μ	0.22
σ_k	1
σ_ϵ	1.3
B_k	$\tilde{\epsilon}/k$
B_ϵ	$C_{\epsilon 2} \tilde{f}_{\epsilon 2}(1/T_s)$
B_{v2}	$6\tilde{\epsilon}/k$
B_f	1
$C_{\epsilon 1}$	$1.4(1+0.05\sqrt{k/v^{\prime 2}})+0.4\exp(-0.1 Re_t)$
$C_{\epsilon 2}$	1.9
$f_{\epsilon 2}$	$[1-0.3 \exp(-Re_t^2)]$
Re_t	$k^2/\nu\tilde{\epsilon}$
L_s	$C_L \max(k^{3/2}/\tilde{\epsilon}, C_\eta \nu^{3/4}/\tilde{\epsilon}^{1/4})$
T_s	$\max(k/\tilde{\epsilon}, 6\sqrt{\nu/\tilde{\epsilon}})$
C_1	1.4
C_2	0.3
C_L	0.23
C_η	70

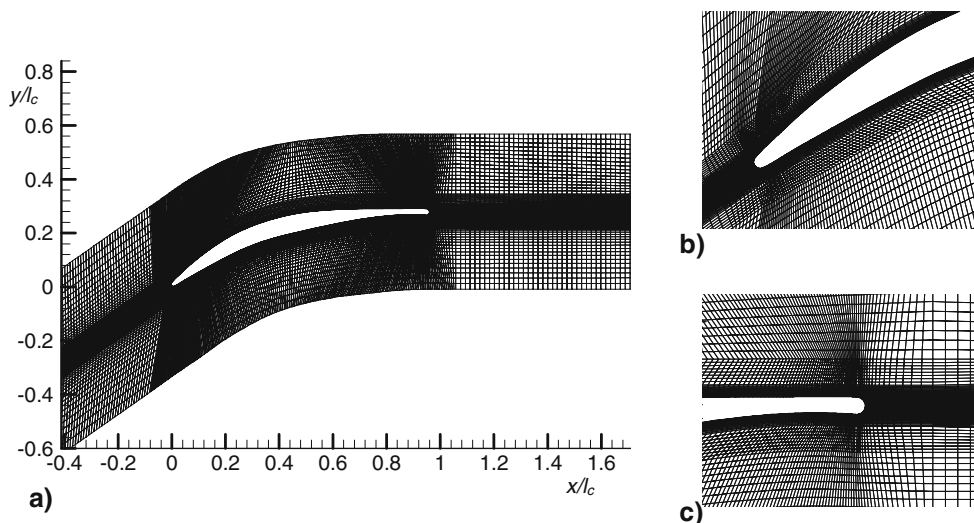


Fig. 6 Controlled-diffusion compressor cascade. **a** computational domain and grid with 27,324 nodes **b** Details of leading edge **c** Details of trailing edge

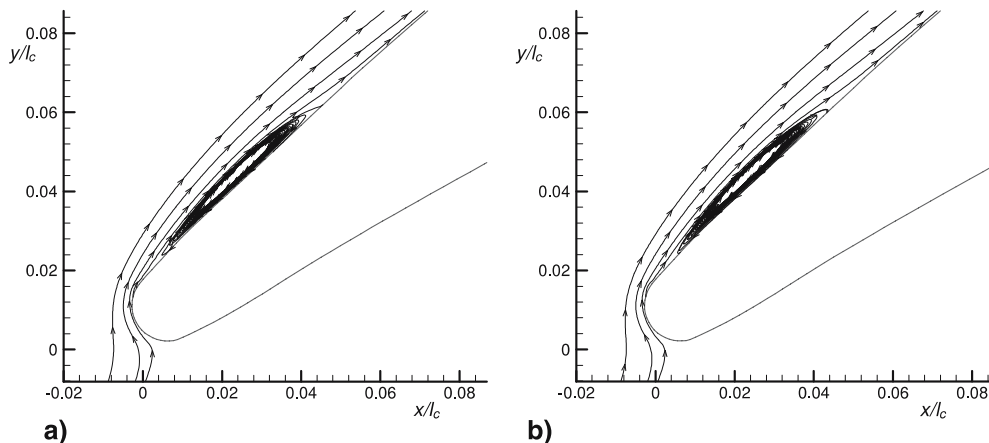


Fig. 7 Controlled-diffusion compressor cascade. Leading-edge separation bubble computed with: **(a)** SUPG+DRDJ, **(b)** V-SGS+DRDJ

the off-design condition with inflow angle $\beta = 46^\circ$ is considered here. Under these conditions the suction side is subjected to a strong adverse pressure gradient, which generates a challenging transitional flow, with a pronounced boundary layer thickening as the trailing edge is approached [12]. The chord Reynolds number, based on the inflow velocity U_{in} ($=85$ m/s), is 7×10^5 . The flow is isothermal and essentially incompressible. Figure 6 shows the mesh used in the computations, which is an H topology grid made of 27,324 nodes, with $(\Delta y^+)_{max} = 1.0$.

The numerical strategy here includes the Pressure-Stabilizing/Petrov–Galerkin formulation [13], which allows equal-order interpolation functions for velocity and pressure. Computations are carried out by solving the coupled equation systems iteratively with the FGMRES technique [14]. The DRDJ enhancement is applied in the context of an advection–reaction equation for k , $\tilde{\epsilon}$ and $\overline{v^2}$, and a diffusion–reaction equation for \tilde{f} . The need for an advanced closure model in this problem was partially due to the complex flow struc-

ture, with a leading-edge separation bubble that could not be resolved with a standard k - ϵ model and a strong adverse pressure gradient characterizing all the boundary layer development.

At the inlet section of the computational domain uniform profiles are used for the velocity components and turbulence quantities. The experimental free-stream distribution is used for the mean velocity profile. The turbulence intensity and the characteristic length scale are:

$$TI = \frac{\sqrt{u'^2}}{U_{in}} = 1.5\%, \quad l_\epsilon/l_c = \frac{\sqrt{k^3}}{\tilde{\epsilon}l_c} = 5.6\% \quad (4.7)$$

Homogeneous Neumann boundary conditions are imposed at the outlet section, and the flow periodicity is imposed at the lower and upper boundaries of the computational domain.

Figure 7 shows the leading-edge streamlines computed with the SUPG+DRDJ and V-SGS+DRDJ formulations. Both results show a separation bubble with a chord-wise length of 6.3 and 6.5% for the SUPG+DRDJ and V-SGS+DRDJ

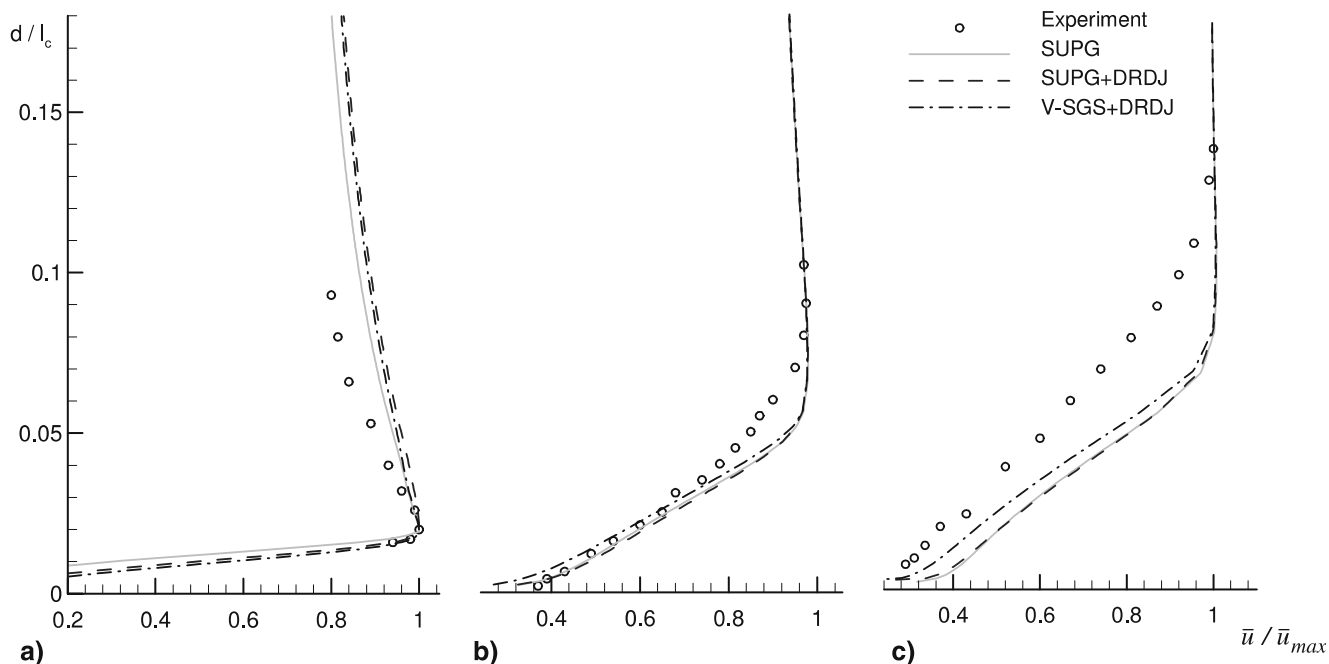


Fig. 8 Controlled-diffusion compressor cascade. Suction-side streamwise velocity profiles at (a) 5.2%, (b) 64% and (c) 95% of the chord

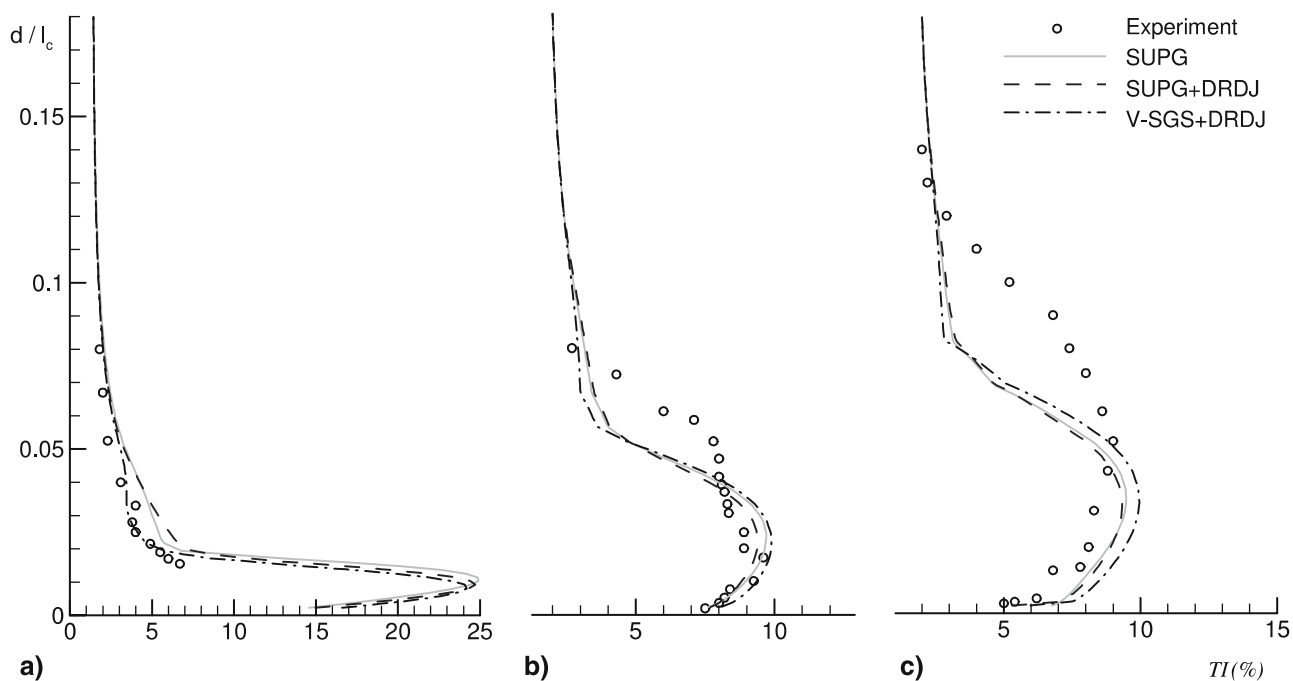


Fig. 9 Controlled-diffusion compressor cascade. Suction-side streamwise turbulence intensity profiles at (a) 5.2%, (b) 64% and (c) 95% of the chord

formulations, respectively, which are in fairly good agreement with the experimentally observed [11] static pressure distribution on the blade suction side. Figures 8 and 9 show the suction-side boundary layer profiles obtained experimentally and with the SUPG, SUPG+DRDJ and V-SGS+DRDJ formulations.

The streamwise velocity and turbulence intensity profiles show reasonably good agreement between the experimental and numerical data. Because of the limitation of the turbulence model, the computed turbulence intensity near the stagnation point at the leading edge is too high. For all three formulations this limitation of the closure model causes the

Table 2 Controlled-diffusion compressor cascade–chordwise evolutions of some of the integrated quantities of the boundary layer

x/l_c	Experiment			SUPG+DRDJ			V-SGS+DRDJ		
	δ^*/l_c	θ^*/l_c	H	δ^*/l_c	θ^*/l_c	H	δ^*/l_c	θ^*/l_c	H
0.052	0.0213	0.0086	2.477	0.0206	0.0069	2.986	0.0184	0.0069	2.667
0.64	0.0491	0.0318	1.544	0.0374	0.0242	1.545	0.0421	0.0257	1.638
0.95	0.1051	0.0581	1.809	0.0594	0.0360	1.650	0.0682	0.0385	1.771

boundary layer to be a little bit thinner compared to the experimental data. Nevertheless all three models are able to resolve the leading edge separation well and capture the turbulence-intensity peak with reasonably good accuracy prior to reaching 64% of the chord.

Figure 9a shows that the V-SGS+DRDJ formulation results in a significant improvement in representing the boundary layers developed under the influence of the leading-edge separation and the induced transitional behavior caused by the high reaction effects [15]. Moving downstream, as it can be seen in Fig. 9b and c, there is substantial agreement between the boundary layer profiles computed by using the SUPG formulation with and without the DRDJ enhancement. This confirms that the SUPG+DRDJ formulation is able to adaptively recover the SUPG behavior where the reaction effects are lower, and thus function without affecting the accuracy where such stabilization enhancements are not needed.

To provide the reader with a more quantitative performance assessment for the SUPG+DRDJ and V-SGS+DRDJ formulations, we report the chord-wise evolutions of some of the integrated quantities of the boundary layer. These integrated quantities are the displacement and momentum thicknesses δ^*/l_c and θ^*/l_c , and the shape factor H . Table 2 shows, for the experiment and the SUPG+DRDJ and V-SGS+DRDJ formulations, these quantities at 5.2, 64 and 95% of the chord.

5 Concluding remarks

A new stabilization enhancement, which we call the DRDJ, has been developed for reaction-dominated flows, starting with the DRD formulation developed earlier. Both the DRD and DRDJ formulations are intended to be used with a core stabilized formulation, such the SUPG or V-SGS method. With test computations for a model problem, we were able to show that the DRD and DRDJ techniques significantly enhance the performance of the SUPG and V-SGS formulations in reaction-dominated flows. Because the closure equations of some of the popular turbulence models involve reaction terms, the stabilization enhancements we described here can be used in more effective modeling of turbulent flows. We demonstrated that by successfully applying the SUPG and V-SGS formulations enhanced with the DRDJ to 2D flow computation in a compressor cascade, where the equations solved are based on the $k-\varepsilon-v^2-f$ turbulence model.

References

- Hauke G (2002) A simple subgrid scale stabilized method for the advection-diffusion-reaction equation. *Comput Methods Appl Mech Eng* 191:2925–2947
- Tezduyar TE, Park YJ (1986) Discontinuity capturing finite element formulations for nonlinear convection-diffusion-reaction equations. *Comput Methods Appl Mech Eng* 59:307–325
- Brooks AN, Hughes TJR (1982) Streamline upwind/Petrov–Galerkin formulations for convection dominated flows with particular emphasis on the incompressible Navier–Stokes equations. *Comput Methods Appl Mech Eng* 32:199–259
- Corsini A, Rispoli F, Santoriello A (2005) A variational multiScale higher-order finite element formulation for turbomachinery flow computations. *Comput Methods Appl Mech Eng* 194:4797–4823
- Lien FS, Kalitzin G, Durbin PA (1998) RANS modeling for compressible and transitional flows. Proceedings of the summer program 1998, Center for Turbulence Research, Stanford University, California pp 267–286
- Corsini A, Rispoli F, Santoriello A (2004) A new stabilized finite element method for advection-diffusion-reaction equations using quadratic elements. *MFF – modelling fluid flow – the state of the art*. Springer, Berlin Heidelberg New York, pp 247–266
- Tezduyar TE (2003) Computation of moving boundaries and interfaces and stabilization parameters. *Int J Numer Methods Fluids* 43:555–575
- Hughes TJR (1995) Multiscale phenomena: Green’s functions, the Dirichlet-to-Neumann formulation, subgrid scale models, bubbles and the origin of stabilized methods. *Comput Methods Appl Mech Eng* 127:387–401
- Hughes TJR, Feijóo GR, Mazzei L, Quincy J-B (1998) The variational multiscale method—a paradigm for computational mechanics. *Comput Methods Appl Mech Eng* 166:3–24
- Durbin PA (1995) Separated flow computations with the $k-\varepsilon-v^2$ model. *AIAA J* 33:659–664
- Elazar Y, Shreeve RP (1990) Viscous flow in a controlled diffusion compressor cascade with increasing incidence. *ASME J Turbomach* 112:256–266
- Chen WL, Lien FS, Leschziner MA (1998) Computational prediction of flow around highly loaded compressor cascade blades with non-linear eddy-viscosity models. *Int J Heat Fluid Flow* 19:307–319
- Tezduyar TE (1992) Stabilized finite element formulations for incompressible flow computations. *Adv App Mech* 28:1–44
- Saad Y (1993) A flexible inner-outer preconditioned GMRES algorithm. *SIAM J Sci Comput* 14:461–469
- Corsini A, Rispoli F, Santoriello A (2005) Quadratic Petrov–Galerkin finite elements for advective–reactive features in turbomachinery CFD. *Int J Numer Methods Heat Fluid Flow* 15(8):894–925
- Hughes TJR, Tezduyar TE (1984) Finite element methods for first-order hyperbolic systems with particular emphasis on the compressible Euler equations. *Comput Methods Appl Mech Eng* 45:217–284